


Pedotransfer functions for converting laser diffraction particle-size data to conventional values

A. MAKÓ^a, G. TÓTH^{a,b} , M. WEYNANTS^c, K. RAJKAI^a, T. HERMANN^b & B. TÓTH^{a,b}

^aHungarian Academy of Sciences ISSAC-CAR, Herman Ottó út 15, Budapest, H-1022, Hungary, ^bDepartment of Crop Production and Soil Science, Georgikon Faculty, University of Pannonia, Deák F. u. 16, Keszthely, H-8360, Hungary, and ^cEuropean Commission, Joint Research Centre (JRC), Via Enrico Fermi 2749, 21027, Ispra, Italy

Summary

The objective of this study was to develop pedotransfer functions (PTFs) for converting soil particle-size distribution (PSD) data from the laser diffraction method (LDM) to the classical sieve–pipette method (SPM) for use on a wide range of temperate soil types. Four hundred soil samples, representative of European soil types and climate zones, were selected from the LUCAS (Land Use/Land Cover Area Frame Survey) topsoil database and their PSDs were determined with LDM and SPM. The LDM measurements were made on samples with (i) their organic matter (OM) removed and (ii) their OM content present. The ranges of PSD obtained with the two pretreatment methods enabled clay–silt and silt–sand boundaries from LDM (6.6 and 60.3 μm for soil with OM, respectively, and 5.8 and 69.2 μm for soil without OM, respectively) to be optimized. Optimization of the boundaries of the fractions considerably improved the prediction performance of SPM PSD from LDM PSD. Specific PTFs with different input requirements were developed for continental scale applications in Europe to convert data from LDM to SPM. The predictions of SPM clay, silt and sand contents were the most accurate with PTFs that used PSD from LDM and soil chemical properties (R^2 0.83, 0.81, 0.94; RMSE 6.14, 7.91 and 6.58%, respectively). For the most accurate results no pretreatment for OM removal was required, but data on chemical properties were necessary. If no soil chemical data are available, the most accurate PTFs need input data of LDM PSD that originate from samples on which the OM content was removed prior to the PSD analysis.

Highlights

- PTFs are developed to harmonize PSD data between laser diffraction (LDM) and sieve–pipette (SPM) methods.
- PTFs are derived from a representative dataset from Europe for application at the continental scale.
- Clay–silt and silt–sand boundaries for LDM without removing OM are at 6.6 and 60.3 μm , respectively.
- Clay–silt and silt–sand boundaries for LDM with OM removed are at 5.8 and 69.2 μm , respectively.

Introduction

Particle-size distribution (PSD) is a fundamental soil physical property that provides information about the size and distribution of soil mass fractions. It is commonly used for soil classification and to characterize soil and geomorphological processes. It affects many other soil properties and can be the basis for estimating soil hydraulic characteristics (Ryzak & Bieganski, 2011; Makó *et al.*, 2014).

Sand-size particles are usually determined by sieving, whereas smaller particles are generally measured by the pipette or

hydrometer methods (Gee & Bauder, 1986). The latter methods are generally used in combination with sieving and are often termed sieve–pipette or sieve–hydrometer methods (SPM or SHM). The sedimentation (pipette or hydrometer) methods are based on Stokes's law, but deviations can be expected when the particles have non-spherical shapes. Most silt-size particles have an irregular shape, and clay-size particles can be platy or tubular in shape (Clifton *et al.*, 1999). The sedimentation methods require relatively large amounts of the sample (20–40 g) and their resolution to subgroups of different sizes is limited. In addition, sedimentation-based procedures are time-consuming, especially for determination of the < 2 μm size fraction.

Correspondence: B. Tóth. E-mail: toth.brigitta@agrar.mta.hu

Received 8 April 2016; revised version accepted 2 June 2017

Laboratories use diverse pretreatments in routine PSD analyses to remove cementing and flocculating agents, especially OM, iron oxides, carbonates and soluble salts (Gee & Bauder, 1986). The results obtained with various pretreatment methods might differ; therefore, the one used must be defined clearly (Shein, 2009). The international SPM standard (ISO 11277: 2009) makes the destruction of OM and the removal of soluble salts and gypsum obligatory, but the removal of other cementing agents is optional. Thereafter, chemical dispersion is prescribed (i.e. saturation of the exchange complex with a strongly electron-negative cation, resulting in a large hydrated radius). Mechanical dispersion is most commonly used in soil-physics laboratories because of the ease and speed of the process. Ultrasonic dispersion uses vibration wave transmission in the soil solution (Genrich & Bremner, 1972).

The laser diffraction method (LDM) is now applied more frequently by soil scientists for the determination of soil PSD (Beuselinck *et al.*, 1998), but it has not yet completely replaced the labour-intensive SPMs or SHMs, which represent the international standards for the particle-size analysis of soil. The principle of LDM for PSD measurement and the description of different diffraction theories is given in de Boer *et al.* (1987). The results obtained with this method are volumetric, which assumes that all particles have a spherical shape and identical densities. The volumetric particle-size distribution calculated concurs with the mass distribution (Ryżak & Bieganski, 2011). The LDM analyses small samples (0.5 g to a few grams) within 5–10 minutes, which makes it suitable for the rapid, accurate analysis of a large number of samples. Recent laser diffractometers provide a wide range of measurements from fractions of micrometres to several millimetres. The drawbacks are the cost of LDM instruments, the difficulty of obtaining samples from the desired grain size for further analysis and the lack of standard operating procedures for soil analysis.

The LDM data might vary according to the type of diffractometer, the amount and state of the sample, the evaluation theory (Fraunhofer or Mie), the defined refractive and absorption indices and the mixing, pumping and sonication dispersion settings (Ryżak & Bieganski, 2011; Sochan *et al.*, 2012; Makó *et al.*, 2014).

Several papers compare LDM PSD data with either SPM (e.g. Beuselinck *et al.*, 1998; Konert & Vandenberghe, 1997; Eshel *et al.*, 2004; Yang *et al.*, 2015) or SHM data (e.g. Ryżak & Bieganski, 2010; Centeri *et al.*, 2015; Fenton *et al.*, 2015). A review of the literature suggests that LDM usually tends to underestimate the clay fraction. This can be attributed mainly to the non-spherical shape of the particles (Fedotov *et al.*, 2007; Polakowski *et al.*, 2014). The latter authors stated that different results might be related to the optical properties selected or measurement limits of earlier equipment. The lack of comparability might also arise from differences in the LDM equipment used, the pretreatments applied and the settings used (Ryżak & Bieganski, 2011; Madarász *et al.*, 2012; Sochan *et al.*, 2012; Makó *et al.*, 2014).

Although previous attempts have been made to construct models for converting LDM data to SPM data, most were based on small datasets representing a selected soil group, pilot area, landscape or watershed. Therefore, the conversion

models might have a restricted use on a national or continental scale.

The aim of this study was to verify model relations between PSDs determined with LDM and SPM for soil types that are representative of the whole European Union. The specific objectives were to: (i) examine differences in PSD data determined by the two methods on a database representing the heterogeneous soil cover of Europe, (ii) demonstrate the effects of pretreatments on the LDM data and (iii) provide prediction models (i.e. pedotransfer functions [PTFs]) to convert LDM data (vol %) to SPM data (mass %) for application in Europe and similar environments.

Materials and methods

The LUCAS soil database

The Land Use/Land Cover Area Frame Survey (LUCAS) is the first consistent spatial database of the soil cover across Europe. Around 22 000 soil samples were collected from 10% of the survey points by standard sampling procedures, and were analysed in a certified laboratory with unified standard methods (Tóth *et al.*, 2013).

Among the LUCAS topsoil samples, 400 were selected to represent the variation and differentiation in soil cover (Table 1). The selection was stratified by texture classes and land cover, followed by simple random sampling in each stratum using the R package *srswor* (Tillé & Matei, 2015). Finally, we verified that the representation of soil characteristics (e.g. organic carbon and calcium carbonate content), climate zones and countries in the selected samples was comparable with that in the full dataset.

Determination of particle-size distribution

The conventional SPM and LDM methods were used to measure the soil PSD. For both methods the soil samples were air-dried, gently crushed and dry-sieved at 2000- μm mesh size. Macroscopic traces of OM (e.g. roots, chaffs and debris) were removed physically.

Prior to SPM analysis, each sample was chemically pretreated with 30% hydrogen peroxide solution to destroy OM in accordance with the ISO 11277:2009 standard. Carbonates and iron oxides were not removed because it is optional in the standard method. Removal of OM was applied to destroy soil aggregates and microaggregates.

To test the effect of OM on the PSD obtained by LDM, two sets of LDM measurements were made. Each of the samples was analysed by the LDM both with and without OM removal (see ISO standard above). After pretreatment, the OM-free suspension was allowed to evaporate at 40°C to complete dryness, then gently crushed and sieved again through a 2000- μm mesh. The two datasets from the LDM PSD data were: 'OM not removed' (OMNR, $n = 809$) and 'OM removed' (OMR, $n = 832$). The 809 and 832 samples of soil represent duplicate, and in some instances triplicate, subsamples of the initial 400 from the LUCAS archive; LDM PSD was measured at least twice or even three times if PSD curves were very different from each other.

Table 1 Mean physical and chemical properties of the soil samples used in the particle-size distribution (PSD) measurements ($N = 400$).

Soil properties	Mean	Standard deviation	Minimum	Maximum
Clay ^a / m %	22.3	15.0	1.0	76.0
Silt ^b / m %	41.7	18.2	4.0	88.0
Sand ^c / m %	36.0	26.2	1.0	94.0
pH(H ₂ O) / –	6.3	1.2	3.8	8.7
pH(CaCl ₂) / –	5.8	1.3	2.8	7.9
OC ^d / g kg ⁻¹	28.6	25.7	3.1	170.3
CaCO ₃ / g kg ⁻¹	47.3	108.2	0.0	607.0
CEC ^e / cmol(+)kg ⁻¹	15.7	11.7	1.0	92.2

^aClay, clay content (<0.002 mm).

^bSilt, silt content (0.002–0.063 mm).

^cSand, sand content (0.063–2.0 mm) (all these fractions were determined by the sieve–pipette method).

^dOC, organic carbon content.

^eCEC, cation exchange capacity.

Laboratory standards are described by Tóth *et al.* (2013).

Sieve–pipette method (SPM). The PSD was determined by a combination of sieving and sedimentation, starting with about 20–30 g (depending on soil texture) air-dried soil (ISO 11277:2009). Particles of 63–2000 µm (sand fraction) were determined by a combination of wet and dry sieving. Particles passing the 63-µm sieve were determined by sedimentation with the pipette method. A particle density of 2650 kg m⁻³ was used to calculate the sedimentation time. ‘Calgon’ (containing 33 g sodium hexametaphosphate and 7 g anhydrous sodium carbonate in 1 l aqueous solution) was used for chemical dispersion. The pretreated suspension was shaken for 18 hours on an end-over-end shaker. The percentages (mass %) of the constituent fractions (sand, 63–2000 µm; silt, 2–63 µm; clay, < 2 µm) were obtained from the PSD analysis.

Laser diffraction method (LDM). A Mastersizer 2000 (Malvern Instruments, Malvern, UK) laser diffractometer, which measures within a size range of 0.02–2000 µm (Mastersizer 2000 User Manual, 1999), was used for LDM analysis (ISO 13320:2009). Measurements were made with a Hydro 2000G dispersion unit.

The PSD was usually determined on two or three replicates (measurement of distinct subsamples) with the LDM. If the shapes of the PSD curves of two repetitions were largely dissimilar, a third measurement was made. The mass of dry soil samples placed into the dispersion unit was in the range of 0.5–1 g depending on the ‘obscuration’ of the soil suspension after dispersion. In this context obscuration is a measure of the amount of the light scattered by the soil particles and correlates with the concentration of measured material present in the laser diffractometer. According to the Mastersizer 2000 manual, the obscuration values should be between 10 and 20%.

Dry soil samples, both with and without OM removal, were placed on a watch glass and moistened by adding drops of standard Calgon solution. Thereafter, the soil paste was washed into the tank of the dispersion unit and a further 25 cm³ of Calgon solution was poured on to it. Laser diffraction measurements were made in ~800 cm³

soil and distilled water suspension (Bieganowski *et al.*, 2010). To ensure complete disaggregation and dispersion the soil suspension was then treated for 240 s with ultrasound at 75% of maximum power (0.75 × 35 W and 0.75 × 40 kHz).

The Hydro 2000G dispersion unit has an integrated stirrer and pump that prevents the sedimentation of particles and ensures circulation of the sample in the measuring system. The pump speed was set at 29.17 Hz (1750 rpm) and the stirrer at 11.67 Hz (700 rpm) (Sochan *et al.*, 2012), which gave maximum homogenization of the suspension in the beaker while eliminating air bubbles from the suspension (Ryżak & Bieganowski, 2011).

The laser light intensity registered on the detectors of the measurement system was converted to PSD according to the Mie theory. The following settings were assumed for the instrument: refraction index of 1.52 and absorption index of 0.1 for the dispersed phase; refraction index of 1.33 for water.

The wavelength of the laser light was 466 nm for blue and 633 nm for red light. All the measurements lasted 60 s (30 s for blue and 30 s for red) (Ryżak & Bieganowski, 2010). The algorithms selected for PSD calculation were: (i) general purpose analysis, which assumes that the sample probably contains a large number of various fractions and (ii) irregular shape ratio, which takes into account that the particles in the samples are not perfect spheres (Mastersizer 2000 User Manual, 1999).

Optimizing LDM fraction boundaries

To obtain laser-diffraction fractions similar to those of SPM, the fraction boundaries detectable by the LDM device that were nearest to standard SPM boundaries (which are at 2 and 63 µm) had to be defined first. These were found at 1.9 and 60.26 µm and referred to as ‘non-modified LDM fraction boundaries’.

Lin’s concordance correlation coefficient (CCC) (Lin, 1989; Lin *et al.*, 2002; Fisher *et al.*, 2017) was calculated between the SPM and LDM PSD data for each dataset to optimize boundaries of the clay, silt and sand fractions in the LDM data. Lin’s CCC measures how well a new set of observations (LDM PSD) reproduce an original set (SPM PSD). The CCC is calculated by multiplying the Pearson correlation coefficient with a bias correction factor. The Pearson correlation coefficient measures how far each observation deviates from the line of best fit, and the bias correction factor is the slope of the line that relates the two measured datasets. Lin’s CCC indicates perfect agreement if its value is 1. The optimized boundaries are referred to as ‘modified LDM fraction boundaries’ hereinafter. From the PSD data obtained by LDM, 14 possible clay fractions were calculated from the upper boundaries with a range of 1.4–10.0 µm (1.4, 1.6, 1.9, 2.2, 2.9, 3.3, 3.8, 4.4, 5.0, 5.8, 6.6, 7.6, 8.7 and 10.0 µm). In the same way, 12 possible sand fractions were calculated from the lower boundaries with a range of 30.2–138.4 µm (30.2, 34.7, 39.8, 45.7, 52.5, 60.3, 69.2, 79.4, 91.2, 104.7, 120.2 and 138.2 µm). The LDM clay, silt and sand fractions calculated with these boundaries were used as independent variables (X) against the dependent variables (Y) of conventional clay, silt and sand fractions measured with SPM (<2.0, 2–63

and 63–2000 μm , respectively). Lin's method was used for the optimization. The best fraction boundaries gave the largest Lin's CCC values.

Methods to estimate SPM PSD data from LDM PSD results

One potential application of the above datasets is to develop conversion pedotransfer functions (PTFs) to obtain conventional SPM data from the more easily measured LDM data, and possibly from other soil properties that are easy to measure. Different types of PTFs were tested to relate the results of SPM and LDM. We focused on predictions based on the information available from LDM measurements and from basic soil analyses. A series of input variables was tested for the development of PTFs.

To select the best prediction model and to decrease uncertainty of the suggested method of estimation, k -fold cross-validation was used (Lamorski *et al.*, 2014). Each of the datasets (OMNR and OMR) was mixed and divided randomly into five equal-sized disjunctive subsets. Thereafter, five pairs of training and test datasets were set up as follows: one subset (test dataset) was omitted and the remaining four subsets were combined to form the training dataset. This procedure was repeated five times to give five datasets for further development of the prediction model, each with a different subset as the test dataset. Models describing the relation between LDM (vol %) and SPM (mass %) data were derived from the training datasets, and their performance was determined on the test datasets. The final PTFs were obtained by selecting the best performing linear regression equation of the five-fold cross-validation approach.

Several publications have indicated that the relation between corresponding LDM and SPM fractions is not linear (e.g. Booth *et al.*, 2003; Yang *et al.*, 2015). Therefore, the linearity of the relations was tested by comparing different types (namely linear, logarithmic, quadratic, cubic and exponential) of model fitting (SPSS, 2004, regression, curve estimation).

Linear regression with backward elimination was used for developing PTFs (SPSS, 2004, regression, linear regression). Separate PTFs were derived to predict SPM clay and silt contents ($\text{clay}_{\text{SPMpred}}$, $\text{silt}_{\text{SPMpred}}$; mass %) from the corresponding LDM PSD fractions (clay_{LDM} , silt_{LDM} ; vol %) determined without or with OM removal. The predicted SPM sand fraction was obtained as follows in all cases:

$$\text{sand}_{\text{SPMpred}} = 100 - (\text{clay}_{\text{SPMpred}} + \text{silt}_{\text{SPMpred}}),$$

where $\text{sand}_{\text{SPMpred}}$, $\text{clay}_{\text{SPMpred}}$ and $\text{silt}_{\text{SPMpred}}$ are the predicted SPM particle-size fractions (mass %). The indirect calculation, whereby $\text{silt}_{\text{SPMpred}}$ was obtained by subtracting the sum of predicted $\text{clay}_{\text{SPMpred}}$ and $\text{sand}_{\text{SPMpred}}$ from 100%, was also tested, but the estimates were not as good.

The input variables used in the analysis are listed below according to their codes in the PTFs:

PTFs1: non-modified LDM size boundaries (clay_{LDM} or silt_{LDM} ; vol %).

PTFs2: modified LDM clay and silt boundaries ($\text{clay}_{\text{LDMmod}}$ or $\text{silt}_{\text{LDMmod}}$; vol %).

PTFs3: $\text{clay}_{\text{LDMmod}}$ or $\text{silt}_{\text{LDMmod}}$ and organic carbon content (OC, g kg^{-1}), calcium carbonate content (CaCO_3 , g kg^{-1}) and soil pH measured in a water–soil suspension ($\text{pH}(\text{H}_2\text{O})$, –).

PTFs4: similar to PTFs3, but also using the modified LDM sand content ($\text{sand}_{\text{LDMmod}}$; vol %).

PTFs5: similar to PTFs4, but predictions were developed for distinct soil texture groups (Di Stefano *et al.*, 2010). The samples were grouped according to the USDA classification based on $\text{clay}_{\text{LDMmod}}$, $\text{silt}_{\text{LDMmod}}$ and $\text{sand}_{\text{LDMmod}}$ contents. To simplify prediction, the samples were merged into four texture groups with wider boundaries: (i) sand and loamy sand, (ii) sandy loam and loam, (iii) silt loam and (iv) silt, sandy clay loam, clay loam, silty clay loam, sandy clay, silty clay and clay soils. These groups represent homogeneous zones on the USDA particle-size triangle.

PTFs6: similar to PTFs4, but transformed soil properties were also used in the regression analysis. Linear, quadratic, reciprocal and common base logarithmic (\log_{10}) forms of the soil properties were used in the regression analysis (Tóth *et al.*, 2015).

PTFs7: similar to PTFs6, but predictions were developed for aggregated soil texture groups similarly to PTFs5.

The performance of PTFs was assessed both on the training and test datasets by the coefficient of determination (R^2) and the root mean square error (RMSE) (mass %) (Equation (1)):

$$\text{RMSE} = \sqrt{\frac{1}{N} \sum_{i=1}^N (y_i - \hat{y}_i)^2}, \quad (1)$$

where y_i represents clay_{SPM} , silt_{SPM} or sand_{SPM} values, \hat{y}_i represents the predicted $\text{clay}_{\text{SPMpred}}$, $\text{silt}_{\text{SPMpred}}$ or $\text{sand}_{\text{SPMpred}}$ values and N is the number of samples.

The mean and standard errors of the R^2 and RMSE values were calculated for each PTF from five repetitions resulting from the five-fold cross-validation replications. The homogeneity of variance was checked with Levene's test. The significance of differences between the prediction methods was evaluated by a one-way analysis of variance (ANOVA) on both the training and test datasets. The distribution of the residuals from the analysis of variance was assessed by Kolmogorov–Smirnov and Shapiro–Wilk tests. The majority of residuals from ANOVA were normally distributed. Fisher's LSD or Tamhane's T2 test, depending on the homogeneity of variances, was used for comparison of the means at the significance level $P = 0.05$.

Samples in the test datasets were classified into textural groups according to the USDA soil-texture triangle (the fact that the USDA classification uses 50 μm as silt–sand boundary, whereas the new ISO standard (ISO 11277:2009) uses 63 μm , could be a minor source of error). The texture classes determined from predicted and measured SPM PSD data were compared with each other. Similarities between the texture classes derived from SPM measurements and the various prediction models were evaluated statistically, as described above, by comparing cases that are identical in terms of soil texture.

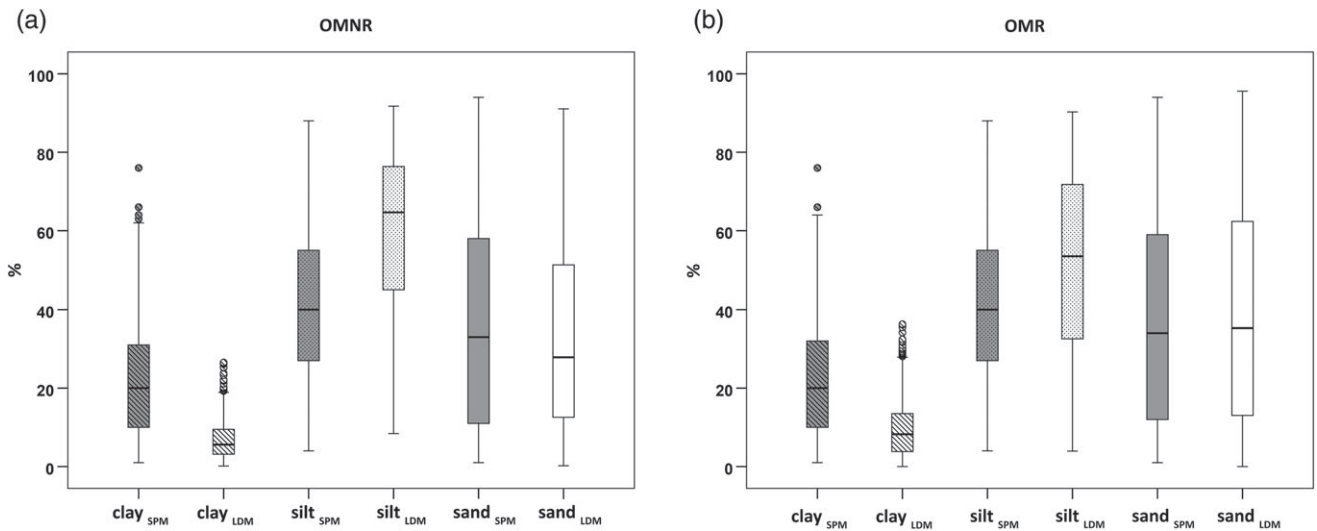


Figure 1 Comparison of the interquartile ranges of soil particle-size fractions measured by different (SPM, sieve-pipette; LDM, laser diffractometer) methods for different pretreatments: (a) OMNR, organic matter not removed; (b) OMR, organic matter removed.

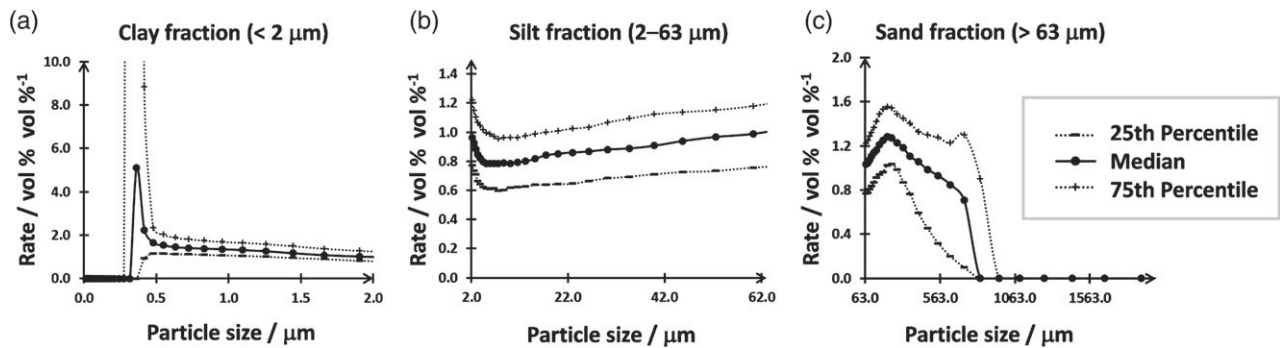


Figure 2 Interquartile ranges of the ratio of the particle volume percentages measured by the two kinds of pretreatments (organic matter not removed and organic matter removed) for size ranges of: (a) clay, (b) silt and (c) sand fractions.

Results and discussion

Comparison of particle-size data and evaluation of OM removal

The soil samples selected show a wide range of variation in several soil properties (Table 1). The boxplots in Figure 1(a,b) show the results of SPM and LPM methods of measurement with and without pretreatment. The mean clay ($< 2 \mu\text{m}$), silt ($2\text{--}63 \mu\text{m}$) and sand ($> 63 \mu\text{m}$) fractions were 22.3, 41.7 and 36.0% for SPM (based on the ISO 11277:2009 standard particle-size limits) and 6.9, 59.8 and 33.3%, respectively, for LDM with OMNR, and 9.6, 51.8 and 38.6%, respectively, for LDM with OMR (Figure 1). The size ranges of the LDM fractions correspond to the ISO size classes for SPM; the equivalent LDM fractions were calculated from the 100 classes by linear interpolation.

The results confirmed that, depending on the sample pretreatment, the LDM underestimated clay content compared with SPM by an average of 69.3% for OMNR and 57.2% for OMR datasets, but overestimated the silt content by an average of 43.5% for OMNR

and 26.2% for OMR datasets. Sand_{LDM} was slightly underestimated (7.4%) for OMNR samples and a little overestimated (5.7%) for OMR samples. The measured fractions also had different interquartile ranges (Figure 1a,b). This corresponds to the findings of other authors (e.g. Konert & Vandenberghe, 1997; Beuselinck *et al.*, 1998; Eshel *et al.*, 2004; Yang *et al.*, 2015).

Figure 1(a,b) shows the differences between the PSDs determined by LDM for different pretreatments. It suggests that the pretreatment slightly altered the ratio of the clay, silt and sand fractions of samples. Figure 2 shows the interquartile ranges of the particle-size ratios (in vol %) measured after the two pretreatments for each LDM size class. Removal of OM results in a larger clay content (ratio > 1) and a smaller silt content (ratio < 1). In the $0.3\text{--}0.5\text{-}\mu\text{m}$ size interval clay content increased after removal of OM. The maximum decline in silt content was at $2\text{--}20 \mu\text{m}$. The sand content increased in the small size ranges ($63\text{--}478 \mu\text{m}$), whereas it decreased in the larger ones ($> 478 \mu\text{m}$). The differences in clay, silt and sand contents measured by LDM for the pretreatments are also reflected in the relations summarized in Figure 3.

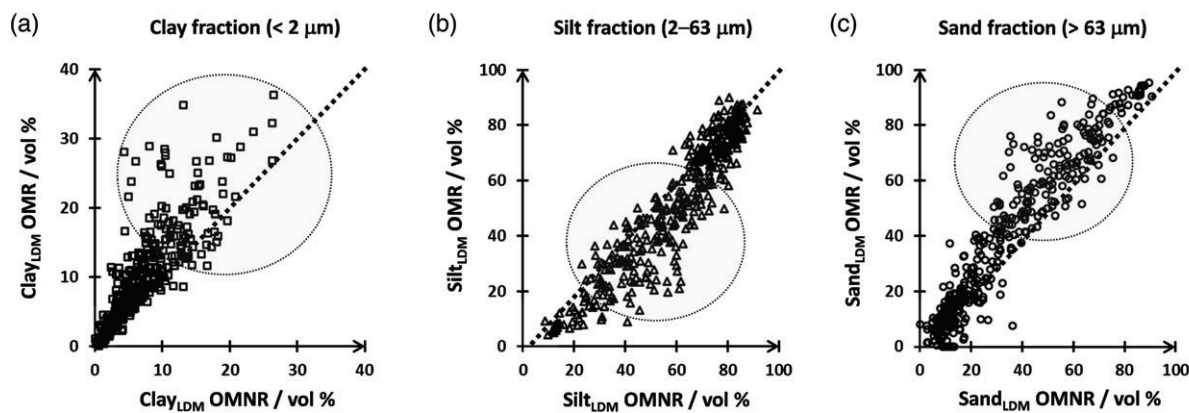


Figure 3 (a) Clay, (b) silt and (c) sand fractions with (OMR) and without (OMNR) organic matter removal by the laser diffractometer method (LDM) (--- shows the 1:1 line). Grey circles represent the problematic ranges of fraction concentration where the largest difference was detected.

Figure 3(a) shows that the differences between the measured clay fractions increase with increasing clay content. The LDM measures smaller silt and larger sand contents, however, after OM removal in the range of samples characterized by medium silt and sand contents; these problematic ranges are indicated with grey circles.

Removal of OM affected the measured PSD considerably, which is contrary to the results of Beuselinck *et al.* (1998). This might be because of the presence of pseudofractions in the particle-size analysis: fine particles are often cemented by organic colloids or organo-mineral colloidal structures into microaggregates that may be resistant to ultrasonic dispersion and Calgon (Fedotov *et al.*, 2007). Part of the clay fraction in these microaggregates probably remains in organo-mineral bonds and the aggregates are measured as silt or sand. Figure 2 also suggests that the sand fraction was affected by the H_2O_2 pretreatment; larger aggregates, which were measured as large sand particles for OMNR, were disrupted in the OMR dataset and the remaining particles were measured as clay, silt and smaller sand particles.

These results contradict those of Di Stefano *et al.* (2010), who found that silt content was not affected by pretreatment. Shein *et al.* (2006), however, confirmed the presence of water-stable microaggregates in the coarse silt (10–50 μm) fraction in a typical Chernozem. They demonstrated their gradual breakdown by different pretreatments and assumed that the stages in the gradual decrease in aggregation depend on soil type (related chemical and physical properties). The disaggregation effect of pretreatment probably also differed for the soil types in our datasets, and without removal of OM part of the clay content remained in closed form in the microaggregates. This possibly explains the large variation in clay contents for the LDM analysis without and with OM removal (Figure 3).

Proposal for modified LDM fraction boundaries

To determine the optimal boundaries between the clay, silt and sand fractions obtained with laser diffractometry, the statistical procedure described by Lin (1989) seemed useful for a wide range of soil types, including those in the LUCAS dataset. The results

of Lin's concordance correlation coefficient (CCC) analyses are summarized in Figure 4.

The optimized boundaries of the clay–silt fraction according to the change in Lin's CCC values are shown in Figure 4a; they are based on a comparison of the clay and silt fractions. For the clay fraction, the CCC value was largest for the 0–6.6 μm fraction with OMNR data and for the 0–5.8 μm fraction with OMR data (CCC: 0.87 and 0.89, respectively) (Figure 4a). Figure 4a also demonstrates that the upper boundaries calculated for clay of 6.6 μm with OMNR and 5.8 μm with OMR data are acceptable as lower boundaries of the silt fraction (CCC: 0.83 and 0.91, respectively). This accords with the results of several authors, which suggest that underestimation of the amount of clay by LDM can be compensated for by changing the clay–silt boundary. Konert & Vandenberghe (1997) determined slightly larger boundary values, 8 μm instead of 2 μm , for randomly selected Dutch soil samples, mostly of fluvial, lacustrine and aeolian origin. The 8- μm clay–silt boundary was also used by Centeri *et al.* (2015) and Fenton *et al.* (2015). Vandecasteele & De Vos (2001) found the 0–6- μm fraction suitable as the clay fraction for LDM of a Belgian soil dataset. Organic matter was removed in both the Dutch and Belgian datasets. Pabst *et al.* (2000) examined the PSDs of kaolin and other clay materials and found that the SPM clay fractions contained clay plates of 3–5 μm . Buurman *et al.* (2001) showed that a separate correlation procedure is required for each type of sediment to obtain the 'real' clay–silt boundary between 2 and 8 μm .

A probable explanation for the larger boundary of the clay–silt fraction could be the slower settling of platy-shaped clay minerals. Consequently, SPM overestimates the clay fraction, whereas LDM underestimates platy particles with random orientations (Ließ *et al.*, 2012). Overestimation of the clay fraction by SPM could also result from diverse particle density. This depends mainly on the mineral composition and humus content, which are usually not taken into account when calculating sedimentation velocity (Eshel *et al.*, 2004).

The different optimal clay–silt boundaries for the OMNR and OMR datasets might be caused by mineralogical changes during

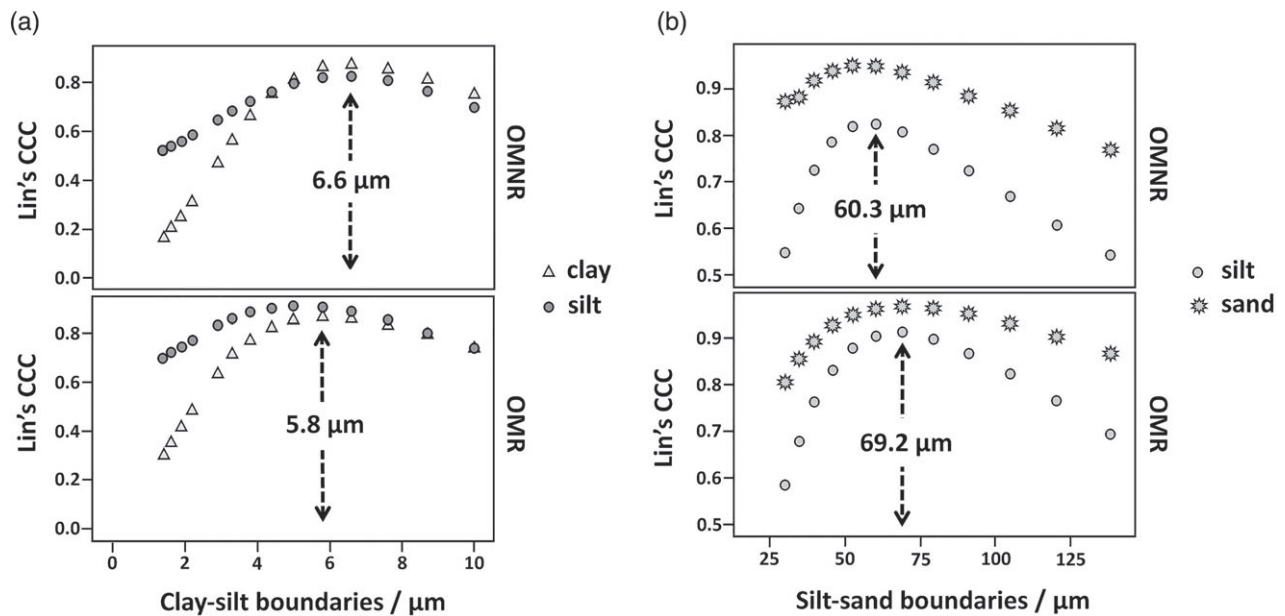


Figure 4 Lin's concordance correlation coefficient (CCC) values of the laser diffractometer methods (LDMs) and sieve-pipette methods (SPMs) (a) clay-silt and (b) silt-sand fraction boundaries measured for the different datasets (OMNR, organic matter not removed; OMR, organic matter removed). The y-axis gives Lin's CCC of the (a) 14 cumulative size classes of the LDM clay (from < 1.4 to < 10.0 μm) and the SPM clay (< 2 μm) fraction and (b) 12 cumulative size classes of the LDM sand (from > 30.2 to > 138.4 μm) and the SPM sand (> 63 μm) fraction.

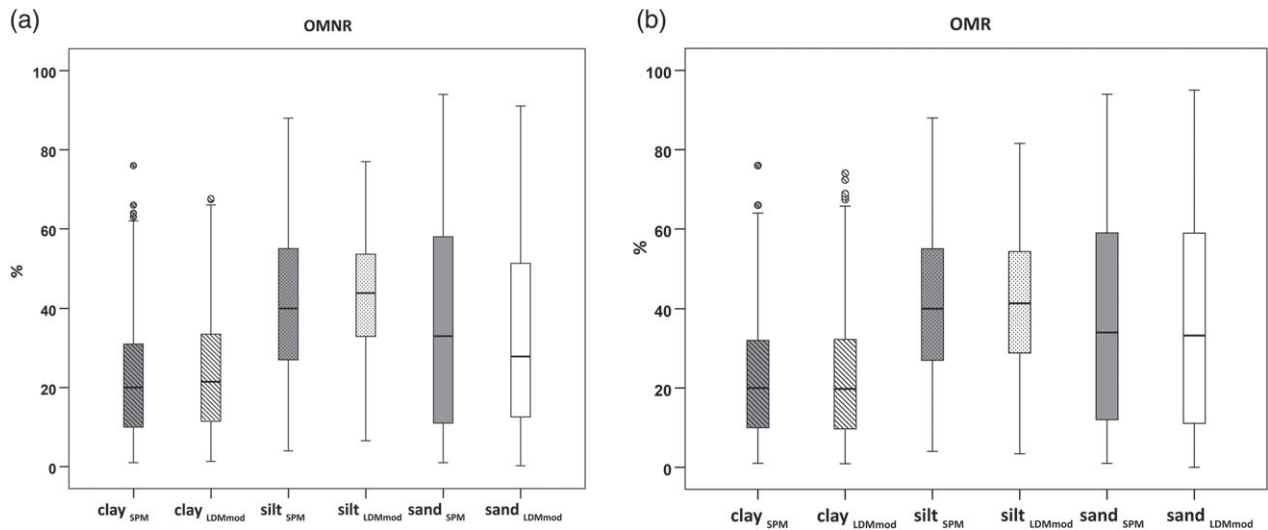


Figure 5 Comparison of the interquartile ranges of soil particle-size fractions measured by different methods (SPM, sieve-pipette; LDM, laser diffractometer) with modified particle-size distribution (PSD) boundaries for different pretreatments: (a) OMNR, organic matter not removed and (b) OMR, organic matter removed. The $\text{clay}_{\text{LDMmod}}$, $\text{silt}_{\text{LDMmod}}$ and $\text{sand}_{\text{LDMmod}}$ indicate the modified fraction boundaries.

pretreatment. Intensive oxidation by H_2O_2 and heating at the end of OM removal may change soil properties considerably (Shein, 2009). Clay minerals, especially those that swell, may be transformed during pretreatment (Balázs *et al.*, 2011) and result in the possible 'erosion' of clay plates, leading to a lower boundary of 5.8 μm . Further research is required to confirm this hypothesis.

Figure 4(b) shows the optimized boundaries for the silt-sand fraction according to Lin's CCC values from a comparison of

the silt and sand fractions. The changes in Lin's CCC values indicate that the largest values (the best matches between the two methods) for the sand fraction are at 60.3–2000 μm for OMNR data and at 69.2–2000 μm for OMR data (CCC: 0.95 and 0.97, respectively) (Figure 4b). Figure 4(b) also shows that the lower boundaries calculated for sand are also acceptable as upper boundaries of the silt fraction (CCC: 0.83 and 0.91, respectively). The scientific explanation for the difference between

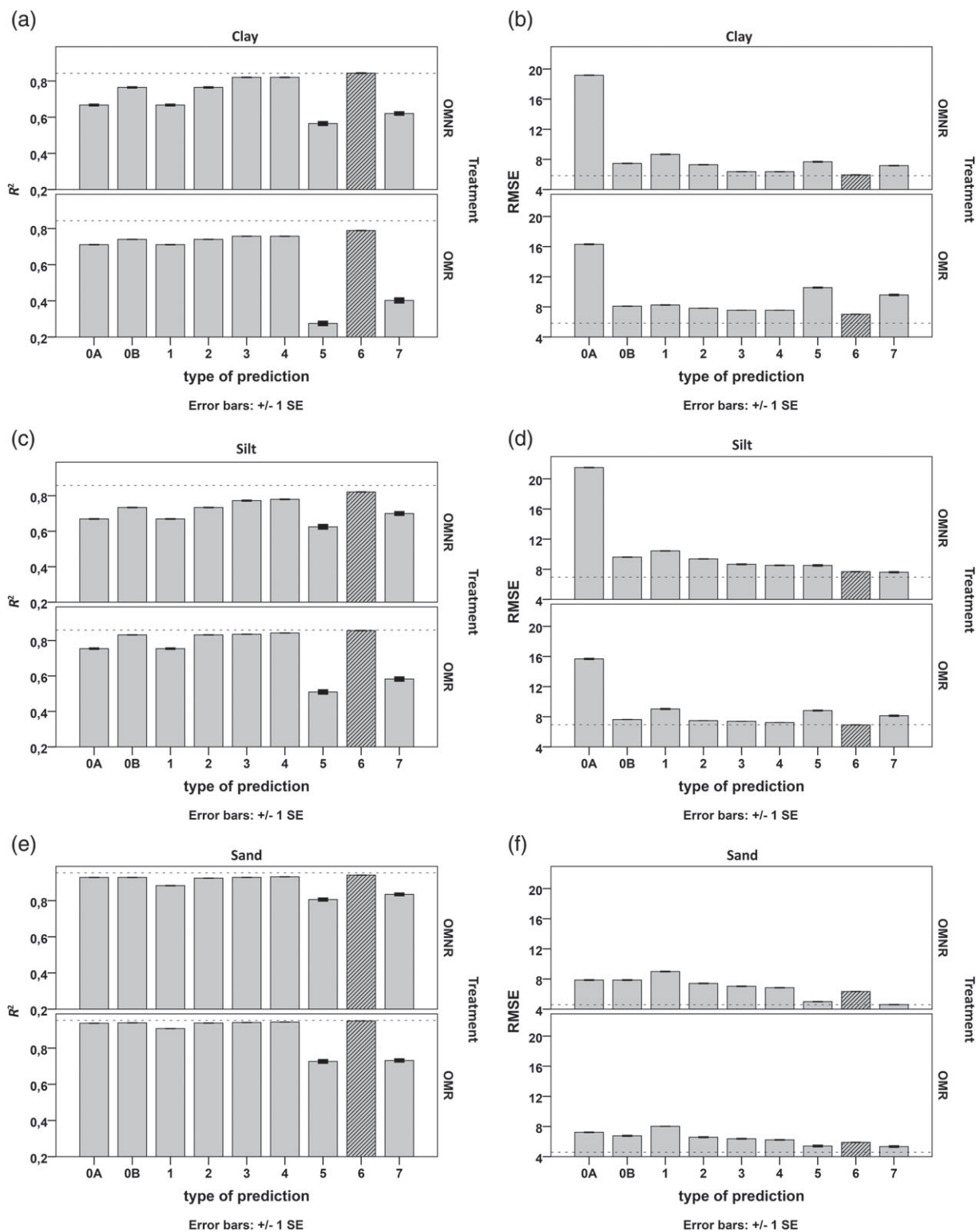


Figure 6 Difference in accuracy of prediction, expressed by R^2 and root mean square error (RMSE) (mass %) for the pedotransfer functions (PTFs) developed for the three particle-size distribution (PSD) fractions, (a) clay, R^2 , (b) clay, RMSE, (c) silt, R^2 , (d) silt, RMSE, (e) sand, R^2 and (f) sand, RMSE, for the different types of pretreatments (OMNR, organic matter not removed; OMR, organic matter removed). Error bars denote ± 1 standard error of the mean for each prediction group. Dotted lines indicate the best level of accuracy and patterned columns indicate the performance of the best conversion model. 0A:PSD_{LDM} is the 'raw' PSD_{LDM} data. 0B:PSD_{SPMpred} is based on PSD_{LDMmod} results. 1–7 represents PTFs 1–7 based on different input parameters described in Materials and methods.

the optimal sand–silt boundaries of OMNR and OMR needs further research.

In the later stages of the statistical analyses, the above clay–silt boundaries (6.6 μm for OMNR and 5.8 μm for OMR) and silt–sand boundaries (60.3 μm for OMNR and 69.2 μm for OMR) were used as ‘modified LDM boundaries’, whereas the ‘non-modified LDM boundaries’ were 2 and 63 μm , respectively.

Figure 5 shows the distribution of PSD derived by SPM and LDM with and without OM pretreatment, and with the modified fraction boundaries for LDM. They show clearly that the amounts of each fraction determined by the different methods are much more similar after modification of the fraction boundary than is the case in Figure 1. The similarity between the SPM (clay_{SPM}, silt_{SPM} and sand_{SPM}) and modified LDM (clay_{LDMmod}, silt_{LDMmod} and sand_{LDMmod}) data is greater for pretreated samples. This is not surprising because pretreatment was also carried out before the SPM measurements.

Pedotransfer functions for converting PSD data from LDM to SPM

The analysis of ‘raw’ SPM and LDM (0A) data and modified LDM_{mod} data (0B) (Figure 6) shows that: (i) pretreatment had a significant, decreasing effect on the RMSE for the clay and silt fractions in the case 0A (OMNR clay: 19.17 ± 0.04 , silt: 21.50 ± 0.05 compared with OMR clay: 16.31 ± 0.07 , silt: 15.68 ± 0.01) (Figure 6b,d), whereas the coefficients of determination (R^2) for the clay and silt fractions slightly increased (OMNR clay: 0.667 ± 0.006 , silt: 0.669 ± 0.003 compared with OMR clay: 0.711 ± 0.002 , silt: 0.754 ± 0.005) (Figure 6a,c), (ii) the RMSE decreased significantly for clay and silt fractions when the fraction boundaries were changed (OMNR 0A clay: 19.17 ± 0.04 , silt: 21.50 ± 0.05 compared with OMNR 0B clay: 7.46 ± 0.05 , silt: 9.61 ± 0.04 ; OMR 0A clay: 16.31 ± 0.07 , silt: 15.68 ± 0.01 compared with OMR 0B clay: 8.09 ± 0.03 , silt: 7.63 ± 0.02) (Figure 6b,d), whereas the modification of LDM PSD boundaries had an increasing effect on R^2 for the clay and silt fractions (OMNR 0A clay: 0.667 ± 0.006 , silt: 0.669 ± 0.003 compared with OMNR 0B clay: 0.765 ± 0.005 , silt: 0.734 ± 0.003 ; OMR 0A clay: 0.711 ± 0.002 , silt: 0.754 ± 0.005 compared with OMR 0B clay: 0.740 ± 0.002 , silt: 0.831 ± 0.002) (Figure 6a,c), (iii) the strongest correlation between SPM and LDM data was for the sand fraction (between 0.928 ± 0.001 and 0.940 ± 0.001) and the weakest was for clay (between 0.667 ± 0.006 and 0.765 ± 0.005) (Figure 6a,c,e), which accords with the results of others (e.g. Ryzak & Bieganowski, 2010; Ließ *et al.*, 2012), and (iv) changing the fraction boundaries resulted in the greatest improvement in R^2 for the clay fraction in OMNR data ($\Delta R^2 = 0.098$) and the silt fraction in OMR data ($\Delta R^2 = 0.077$) (Figure 6a,c).

Linear regression was used to develop the conversion models further (Tables S1 and S2, Supporting Information). A comparison of the performance of conversion models (PTFs) showed that combining LDM_{mod} and routine soil data (OC, CaCO₃,

pH(H₂O)) as input parameters in the model (PTFs6) gave the most accurate prediction results; they have the smallest RMSE (OMNR clay: 5.94 ± 0.04 , silt: 7.68 ± 0.04 ; OMR clay: 7.02 ± 0.03 , silt: 6.92 ± 0.03) (Figure 6b,d) and the largest R^2 values (OMNR clay: 0.844 ± 0.003 , silt: 0.821 ± 0.002 ; OMR clay: 0.789 ± 0.002 , silt: 0.856 ± 0.002) (Figure 6a,c). On the other hand, the proposed PTFs were able to eliminate the effect of OM removal on the efficiency of estimation. With the best prediction method, PTFs6, larger R^2 and smaller RMSE values were achieved for OMNR than for OMR. Preliminary grouping did not improve the accuracy of prediction with PTFs5 and 7. (The comparison of different PTFs with ANOVA is shown in Table S3 in Supporting Information.)

When the accuracy of PTFs 1–7 was tested with independent variables only that were close to normally distributed, there was a decrease in accuracy.

The PTFs that gave the most accurate predictions for the training datasets (PTFs 4 and 6) were included in further analysis. The performance of potential PTFs on the test datasets is shown in Figure 7 and the results of ANOVA in Table S4 in Supporting Information. Use of all transformed and untransformed independent variables (PTFs6) significantly improved the accuracy of the models compared with PTFs4, which include untransformed input variables only. The performance of PTFs 4 and 6 on test datasets, however, was similar based on R^2 (Figure 7a,c,e) and RMSE (Figure 7b,d,f) values.

Removal of OM before LDM measurements, however, did have a noteworthy effect on the performance of the models. The PTFs derived from OMNR performed significantly better, for example the R^2 and RMSE values for clay_{SPMpred} estimated by PTF6 were significantly better for OMNR ($R^2 = 0.832 \pm 0.012$ and RMSE = $6.14 \pm 0.18\%$ for PTFs6) than for OMR ($R^2 = 0.780 \pm 0.007$ and RMSE = $7.30 \pm 0.10\%$).

The distribution of soil texture within the USDA textural triangle for ‘raw’ SPM and LDM data, the modified fraction boundary data and the particle-size data predicted by the best performing PTFs6 are shown in Figure 8. Removal of OM only did not result in the convergence of soil texture distributions (Figure 8a,c). Changes in soil fraction boundaries, however, resulted in a much greater improvement in the correspondence of the texture distribution between SPM and LDM (Figure 8b,d). Figure 8(e,f) shows that the PTFs gave the closest agreement between the distributions of texture determined by SPM and LDM.

The textural triangles (Figure 8) illustrate the distribution of textures in the total soil database, but the test datasets only were used to compare the texture classes formed in different ways. The predicted texture classes estimated by the better performing PTFs only (PTFs1, 2, 4 and 6) were compared with the measured texture classes determined by SPM. The USDA texture classes agreed well with $62.18 \pm 1.98\%$ and $62.10 \pm 2.24\%$ of the measured and predicted values when PTFs6 were applied (Figure 9). This was the largest percentage of matches, but there were no statistically justified differences between the estimation of texture by PTFs2 ($58.60 \pm 0.66\%$ and $57.80 \pm 0.82\%$), PTFs4 ($59.46 \pm 1.58\%$ and

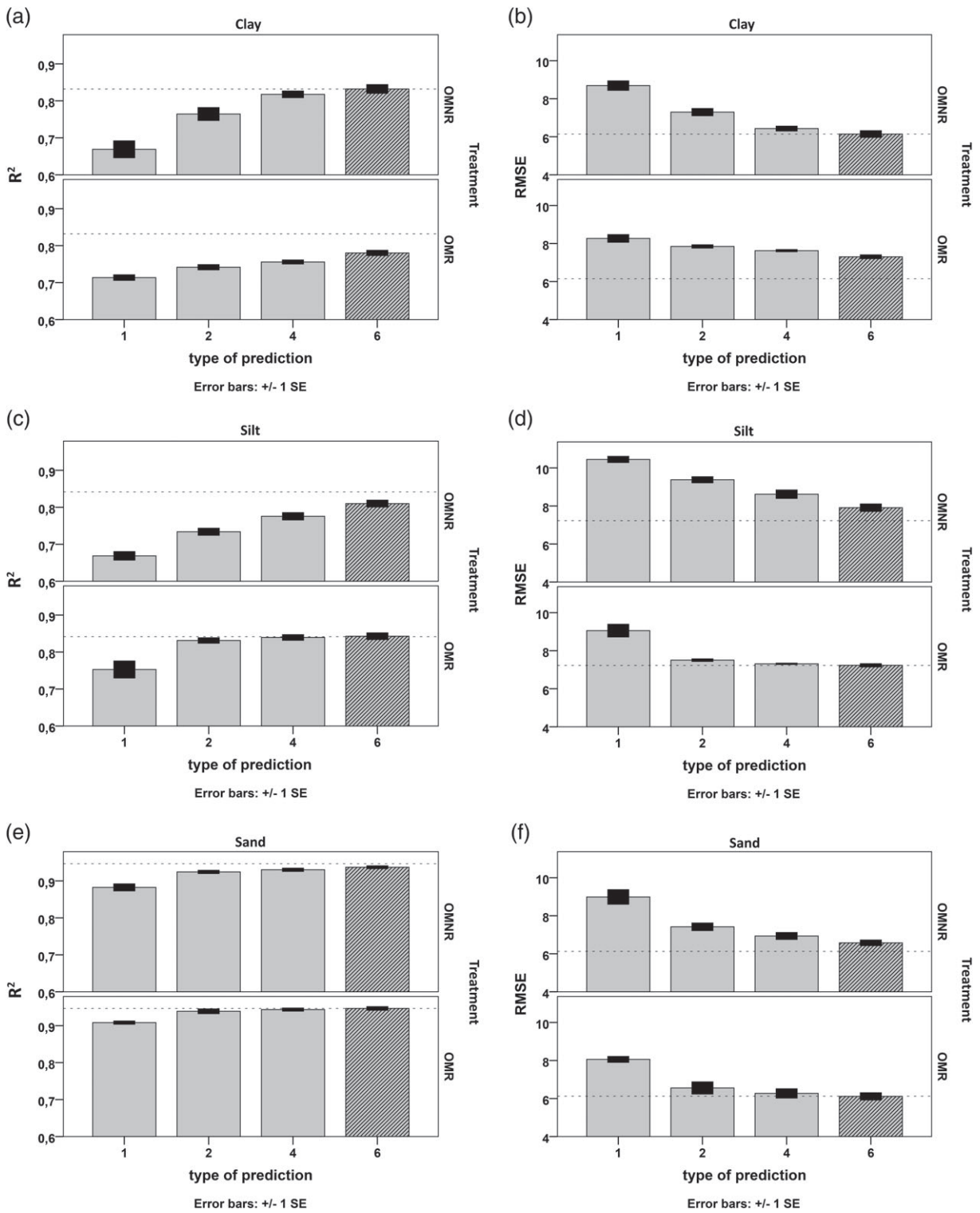


Figure 7 Difference in performance of predictions on test datasets, expressed by R^2 and root mean square error (RMSE) (mass %), for the pedotransfer functions (PTFs) developed for the three particle-size distribution (PSD) fractions, (a) clay, R^2 , (b) clay, RMSE, (c) silt, R^2 , (d) silt, RMSE, (e) sand, R^2 and (f) sand, RMSE, for the different types of pretreatments (OMNR, organic matter not removed; OMR, organic matter removed). Error bars denote ± 1 standard error of the mean for each prediction group. Dotted lines indicate the best level of performance and patterned columns indicate the performance of the best conversion model. 1–4 represents PTFs 1, 2, 4 and 6 based on different input parameters described in Materials and methods.

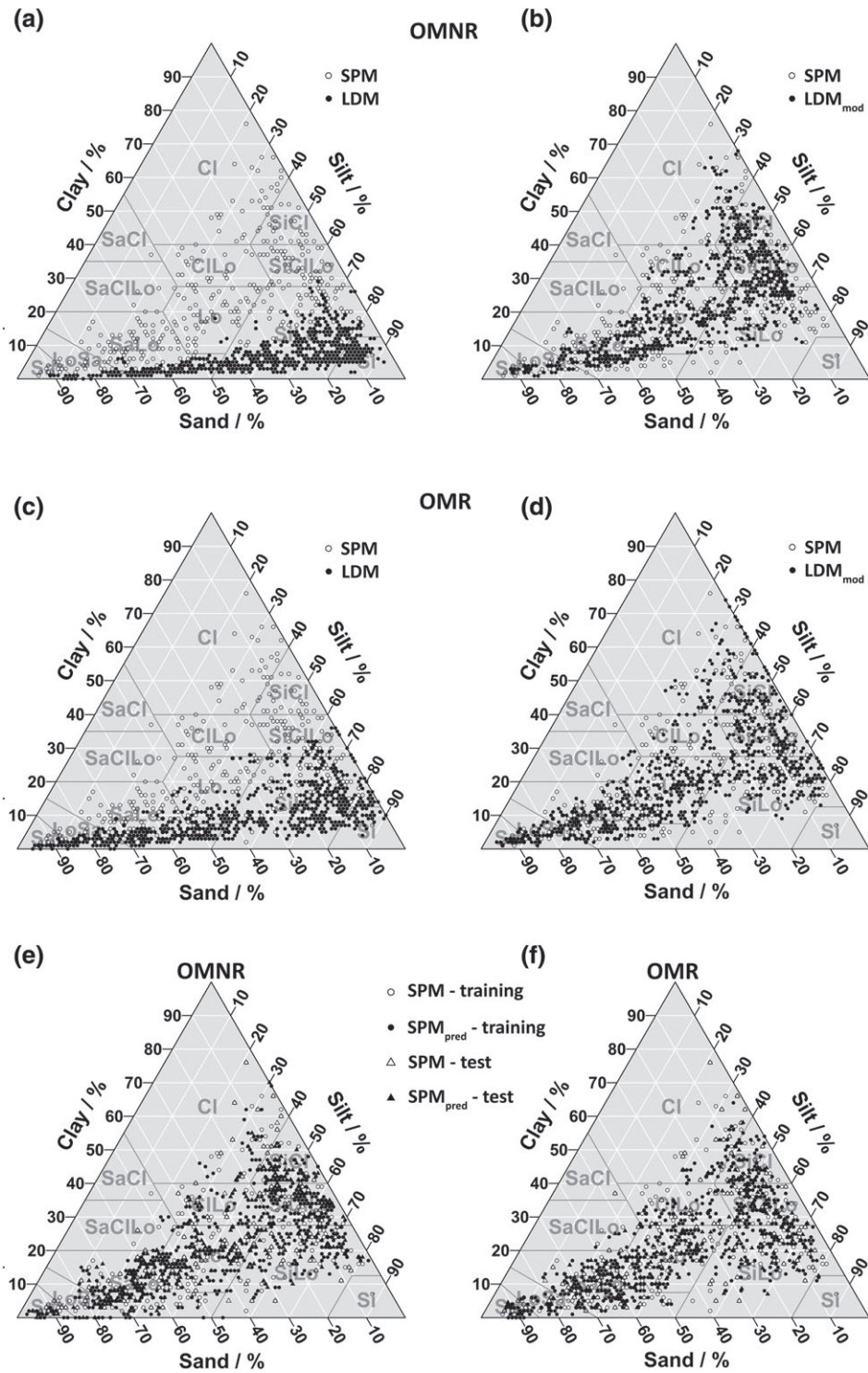


Figure 8 Distribution of soil textures in the USDA textural triangles: (a) measured by sieve–pipette (SPM) and laser diffractometer (LDM) methods for the OMNR (organic matter not removed) dataset, (b) measured by SPM and LDM with modified fraction boundaries for the OMNR dataset, (c) measured by SPM and LDM for the OMR (organic matter removed) dataset, (d) measured by SPM and LDM with modified fraction boundaries for the OMR dataset, (e) measured by SPM and converted LDM for pedotransfer functions (PTFs) 6 with the OMNR dataset and (f) measured by SPM and converted LDM for PTFs6 with the OMR dataset.

Table 2 Recommended conversion pedotransfer functions (PTFs) for continental scale applications in Europe.

Input data options	Number of PTFs	Prediction models ^a
Based on samples without removal of organic matter during pretreatment (OMNR)		
PSD ^b only	2a	$\text{clay}_{\text{SPMpred}} = 0.69 + 0.92 \times \text{clay}_{\text{LDMmod}}$ $\text{silt}_{\text{SPMpred}} = -6.10 + 1.10 \times \text{silt}_{\text{LDMmod}}$
PSD + chemical soil properties	6a	$\text{clay}_{\text{SPMpred}} = 187.40 - 0.055 \times \text{CaCO}_3 + 0.008 \times \text{clay}_{\text{LDMmod}}^2 + 0.002 \times \text{sand}_{\text{LDMmod}}^2 - 0.001 \times \text{OC}^2 - 47.33 \times \sqrt{\text{pH}(\text{H}_2\text{O})} + 15.74 \times \sqrt{\text{OC}} + 1.82 \times \sqrt{\text{CaCO}_3} + 37.85 \times 1/\text{clay}_{\text{LDMmod}} - 359.48 \times 1/\text{pH}(\text{H}_2\text{O}) - 168.57 \times 1/\text{OC} - 0.012 \times 1/\text{CaCO}_3 + 41.59 \times \log_{10} \text{clay}_{\text{LDMmod}} - 90.26 \times \log_{10} \text{OC} - 4.70 \times \log_{10} \text{CaCO}_3$ $\text{silt}_{\text{SPMpred}} = -170.55 + 0.036 \times \text{CaCO}_3 + 0.003 \times \text{silt}_{\text{LDMmod}}^2 + 0.003 \times \text{sand}_{\text{LDMmod}}^2 + 10.94 \times \sqrt{\text{silt}_{\text{LDMmod}}} + 54.02 \times \sqrt{\text{pH}(\text{H}_2\text{O})} + 1.29 \times \sqrt{\text{OC}} - 0.62 \times \sqrt{\text{CaCO}_3} - 107.33 \times 1/\text{sand}_{\text{LDMmod}} + 421.51 \times 1/\text{pH}(\text{H}_2\text{O}) - 34.11 \times \log_{10} \text{sand}_{\text{LDMmod}} - 20.12 \times \log_{10} \text{OC}$
Based on samples undergoing pretreatment including removal of organic matter (OMR)		
PSD only	2b	$\text{clay}_{\text{SPMpred}} = 3.09 + 0.87 \times \text{clay}_{\text{LDMmod}}$ $\text{silt}_{\text{SPMpred}} = 2.41 + 0.93 \times \text{silt}_{\text{LDMmod}}$
PSD + chemical soil properties	6b	$\text{clay}_{\text{SPMpred}} = -44.22 + 0.24 \times \text{sand}_{\text{LDMmod}} - 0.079 \times \text{CaCO}_3 + 0.001 \times \text{OC}^2 + 12.02 \times \text{CaCO}_3 - 2.48 \times \sqrt{\text{clay}_{\text{LDMmod}}} + 13.27 \times \sqrt{\text{sand}_{\text{LDMmod}}} - 0.81 \times \sqrt{\text{pH}(\text{H}_2\text{O})} + 2.30 \times \sqrt{\text{OC}} - 22.95 \times 1/\text{pH}(\text{H}_2\text{O}) - 0.02 \times 1/\text{OC} - 13.79 \times 1/\text{CaCO}_3 + 3.73 \times \log_{10} \text{clay}_{\text{LDMmod}} - 7.05 \times \log_{10} \text{OC}$ $\text{silt}_{\text{SPMpred}} = -26.76 - 0.34 \times \text{sand}_{\text{LDMmod}} - 0.076 \times \text{CaCO}_3 + 0.01 \times \text{silt}_{\text{LDMmod}}^2 + 0.0001 \times \text{CaCO}_3^2 + 2.92 \times \sqrt{\text{sand}_{\text{LDMmod}}} - 3.98 \times \sqrt{\text{OC}} + 0.82 \times \sqrt{\text{CaCO}_3} + 42.77 \times 1/\text{pH}(\text{H}_2\text{O}) + 70.45 \times 1/\text{OC} + 13.48 \times \log_{10} \text{silt}_{\text{LDMmod}} - 2.87 \times \log_{10} \text{sand}_{\text{LDMmod}} + 29.83 \times \log_{10} \text{OC}$

^aclay_{SPMpred}, sieve–pipette method (SPM) clay content (mass %); silt_{SPMpred}, SPM silt content (mass %); clay_{LDMmod}, modified laser diffractometer method (LDM) clay content (vol %); silt_{LDMmod}, modified LDM silt content (vol %); sand_{LDMmod}, modified LDM sand content (vol %); CaCO₃, calcium carbonate content (g·kg⁻¹); OC, organic carbon content (g·kg⁻¹); pH(H₂O), soil pH measured in water–soil suspension (–).

^bPSD, elements of particle size distribution, clay or silt content (mass%).

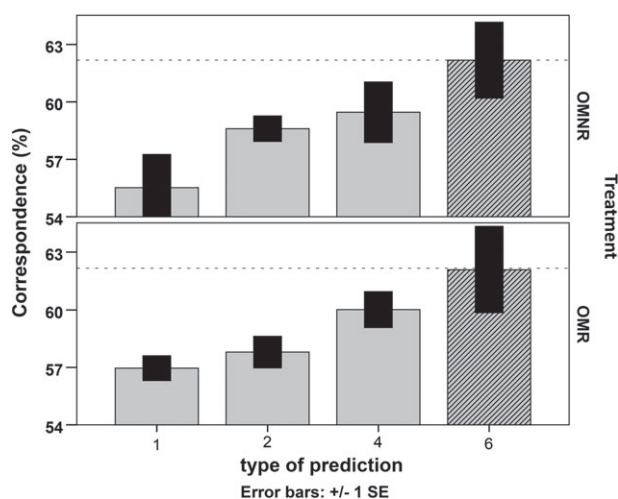


Figure 9 Comparison of the accuracy of assigning samples correctly to the USDA textural class for the measured and predicted values. The differences in correspondence are presented for the pedotransfer functions (PTFs) developed and the different types of pretreatments (OMNR, organic matter not removed; OMR, organic matter removed). Error bars denote ± 1 standard error of the mean for each prediction group and have the same format as in the other figures. Dotted lines indicate the performance of the best conversion model. 1–4 represents PTFs 1, 2, 4 and 6 based on different input parameters described in Materials and methods.

$60.02 \pm 0.94\%$) and PTFs 6 (Figure 9 and Table S5 in Supporting Information).

Conclusions and recommendations

- The PTFs presented to convert PSD data from LDM (vol %) to SPM (mass %) for comparison and harmonization of data are reliable tools for application in Europe.
- New standards for LDM clay–silt boundaries and silt–sand boundaries presented above provide a proper basis for the transformation of LDM PSD to SPM PSD.
- The new PTFs to convert PSD data from LDM (vol %) to SPM (mass %) use the modified particle-size LDM fractions and some optional basic soil chemical data such as OC, CaCO₃ and pH_(H₂O). The use of soil chemical properties as input parameters significantly improved the prediction of SPM PSD from LDM PSD.
- We recommend two sets of PTFs developed on a representative European dataset: (i) one set derived from samples with pretreatment to remove OM (OMR) and (ii) a second set derived from samples for which the OM was not removed (OMNR).
- When data on soil chemical properties, such as OC, CaCO₃ and pH_(H₂O), are available, PTFs that use data from OMNR PSD measurements have similar prediction power to those that use

PSD data with OMR pretreatment. Thus, the time-consuming pretreatment to remove OM cannot be justified in these cases.

- Performance of the conversion with the PTFs depends greatly on the preparation and specifications of the LDM PSD method. To secure reliable and coherent results, standardization of pretreatments and settings for soil LDM PSD measurements is required.
- The continental scale PTFs obtained with the conversion methods developed can be improved further with local databases including soil type, land use, soil management, and so on.
- The following PTFs are recommended for converting PSD from LDM (vol %) to SPM data (mass %) with different pretreatments and input variables (as listed in Table 2):

1 For datasets where PSD data (clay or silt content) only are available, functions in ‘PTFs type 2’ are recommended for data harmonization:

- Function 2a when sample pretreatment did not include the removal of OM.
- Function 2b when sample pretreatment included removal of OM.

2 For datasets where OC, CaCO₃ content and pH_(H₂O) are also known, the best performing functions were those in ‘PTFs type 6’.

- Function 6a when sample pretreatment did not include the removal of OM.
- Function 6b when sample pretreatment included removal of OM.

Supporting Information

The following supporting information is available in the online version of this article:

File S1. Statistical approaches.

Table S1. The effect of fitting method on the accuracy of pedotransfer functions (PTFs) fit. Summary results of R^2 values from ANOVA.

Table S2. Comparison of the different regression models for converting laser diffractometer method (LDM) particle-size distribution (PSD) to sieve–pipette method (SPM) with the variation in R^2 values for the type of models. Results are given as mean of five replicates \pm standard error.

Table S3. The effect of prediction methods (pedotransfer functions, PTFs) on the accuracy of conversion from laser diffractometer method (LDM) to sieve–pipette method (SPM). Summary results for R^2 and root mean square error (RMSE) values from ANOVA.

Table S4. The effect of prediction methods (pedotransfer functions, PTFs) on the performance of conversion from LDM to SPM on test datasets. Summary results for R^2 and RMSE values from ANOVA.

Table S5. The effect of prediction methods (PTFs) on the accuracy of assigning samples correctly to the USDA texture class for the measured and predicted values. Summary results for correspondence (%) values from ANOVA.

Acknowledgements

This research programme was supported by the Hungarian National Research Foundation (OTKA, Grant No. K 119475). The authors would like to thank Sándor Kabos for advice on statistical analyses. We are grateful to the editor-in-chief, associate editor and reviewers for helpful comments on this paper.

References

- Balázs, R., Németh, T., Makó, A., Kovács Kis, V. & Keresztes, M. 2011. Soil mineralogical effects of FAO pre-treatment procedure during the particle size distribution measurements. In: *Sustainability and Competitiveness. Proceedings of the 53rd Georgikon Days, Keszthely* (ed. G. Lukács), pp. 29–30. University of Pannonia Georgikon Faculty, Keszthely.
- Beuselinck, L., Govers, G., Poesen, J., Degraer, G. & Froyen, L. 1998. Grain-size analysis by laser diffractometry: comparison with the sieve-pipette method. *Catena*, **32**, 193–208.
- Bieganowski, A., Ryżak, M. & Witkowska-Walczak, B. 2010. Determination of soil aggregate disintegration dynamics using laser diffraction. *Clay Minerals*, **45**, 23–34.
- de Boer, G.B., de Weerd, C., Thoennes, D. & Goossens, H.W. 1987. Laser diffraction spectrometry: Fraunhofer versus Mie scattering. *Particle Characterization*, **4**, 14–19.
- Booth, C.A., Fullen, M.A., Jankauskas, B. & Jankauskienė, G. 2003. International calibration of the textural properties of Lithuanian eutric albeluvisols. *Soil Science & Agrochemistry*, **4**, 3–10.
- Buurman, P., Pape, T., Reijneveld, J.A., de Jong, F. & van Gelder, E. 2001. Laser-diffraction and pipette-method grain sizing of Dutch sediments: correlations for fine fractions of marine, fluvial, and loess samples. *Netherlands Journal of Geosciences*, **80**, 49–57.
- Centeri, C., Jakab, G., Szabó, S., Farsang, A., Barta, K., Szalai, Z. *et al.* 2015. Comparison of particle-size analyzing laboratory methods. *Environmental Engineering & Management Journal*, **14**, 1125–1135.
- Clifton, J., McDonald, P., Plater, A. & Oldfield, F. 1999. An investigation into the efficiency of particle size separation using Stokes’ law. *Earth Surface Processes & Landforms*, **24**, 725–730.
- Di Stefano, C., Ferro, V. & Mirabile, S. 2010. Comparison between grain-size analyses using laser diffraction and sedimentation methods. *Biosystems Engineering*, **106**, 205–215.
- Eshel, G., Levy, G.J., Mingelgrin, U. & Singer, M.J. 2004. Critical evaluation of the use of laser diffraction for particle-size distribution analysis. *Soil Science Society of America Journal*, **68**, 736–743.
- Fedotov, G.N., Shein, E.V., Putlynev, V.I., Arkhangel’skaya, T.A., Eliseev, A.V. & Milanovskii, E.Y. 2007. Physicochemical bases of differences between the sedimentometric and laser diffraction techniques of soil particle-size analysis. *Eurasian Soil Science*, **40**, 281–288.
- Fenton, O., Vero, S., Ibrahim, T.G., Murphy, P.N.C., Sherriff, S.C. & Huallacháin, D.Ó. 2015. Consequences of using different soil texture determination methodologies for soil physical quality and unsaturated zone time lag estimates. *Journal of Contaminant Hydrology*, **182**, 16–24.
- Fisher, P., Aumann, C., Chia, K., O’Halloran, N. & Chandra, S. 2017. Adequacy of laser diffraction for soil particle size analysis. *PLoS ONE*, **12**, e0176510.
- Gee, G.W. & Bauder, J.W. 1986. Particle-size analysis. In: *Methods of Soil Analysis. Part 1. Physical and Mineralogical Methods* (ed. A. Klute), pp. 383–411. American Society of Agronomy, Madison, WI.

- Genrich, D.A. & Bremner, J.M. 1972. A reevaluation of the ultrasonic vibration method of dispersing soils. *Soil Science Society of America Proceedings*, **36**, 944–947.
- ISO 11277 2009. *Soil Quality – Determination of Particle Size Distribution in Mineral Soil Material – Method by Sieving and Sedimentation*. ISO, Geneva.
- Konert, M. & Vandenberghe, J. 1997. Comparison of laser grain size analysis with pipette and sieve analysis: a solution for the underestimation of the clay fraction. *Sedimentology*, **44**, 523–535.
- Lamorski, K., Bieganski, A., Ryzak, M., Sochan, A., Sławiński, C. & Stelmach, W. 2014. Assessment of the usefulness of particle size distribution measured by laser diffraction for soil water retention modelling. *Journal of Plant Nutrition & Soil Science*, **177**, 803–813.
- Ließ, M., Glaser, B. & Huwe, B. 2012. Uncertainty in the spatial prediction of soil texture. Comparison of regression tree and random forest models. *Geoderma*, **170**, 70–79.
- Lin, L. 1989. A concordance correlation coefficient to evaluate reproducibility. *Biometrics*, **45**, 255–268.
- Lin, L., Hedayat, A.S., Sinha, B. & Yang, M. 2002. Statistical methods in assessing agreement. *Journal of the American Statistical Association*, **97**, 257–270.
- Madarász, B., Jakab, G., Szalai, Z. & Juhos, K. 2012. Examination of sample preparation methods for the laser grain size analysis of soils with high organic matter content. (In Hungarian). *Agrokémia és Talajtan*, **61**, 381–398.
- Makó, A., Rajkai, K., Hernádi, H. & Hauk, G. 2014. Comparison of different settings and pre-treatments in soil particle-size distribution measurement by laser-diffraction method. *Agrokémia és Talajtan*, **63**, 19–28.
- Malvern Instruments Ltd. 1999. *Malvern Operators Guide Mastersizer 2000 User Manual*. Malvern Instruments Ltd., Malvern.
- Pabst, W., Kunes, K., Havrda, J. & Gregorova, E. 2000. A note on particle size analyses of kaolins and clays. *Journal of the European Ceramic Society*, **20**, 1429–1437.
- Polakowski, C., Sochan, A., Bieganski, A., Ryzak, M., Földényi, R. & Tóth, J. 2014. Influence of the sand particle shape on particle size distribution measured by laser diffraction method. *International Agrophysics*, **28**, 195–200.
- Ryzak, M. & Bieganski, A. 2010. Determination of particle size distribution of soil using laser diffraction – Comparison with areometric method. *International Agrophysics*, **24**, 177–181.
- Ryzak, M. & Bieganski, A. 2011. Methodological aspects of determining soil particle-size distribution using the laser-diffraction method. *Journal of Plant Nutrition & Soil Science*, **174**, 624–633.
- Shein, E.V. 2009. The particle-size distribution in soils: problems of the methods of study, interpretation of the results, and classification. *Eurasian Soil Science*, **42**, 284–291.
- Shein, E.V., Milanovskii, E.Y. & Molov, A.Z. 2006. The effect of organic matter on the difference between particle-size distribution data obtained by the sedimentometric and laser diffraction methods. *Eurasian Soil Science*, **39**, S84–S90.
- Sochan, A., Bieganski, A., Ryzak, M., Dobrowolski, R. & Bartmiński, P. 2012. Comparison of soil texture determined by two dispersion units of Mastersizer 2000. *International Agrophysics*, **26**, 99–102.
- SPSS 2004. *SPSS for Windows, Version 13.0*. SPSS Inc., Chicago, IL.
- Tillé, Y. & Matei, A. 2015. *Sampling: Survey Sampling*. R Package version 2.7. [WWW document]. URL <https://CRAN.R-project.org/package=sampling> [accessed on 27 October 2016].
- Tóth, B., Weynants, M., Nemes, A., Makó, A., Bilas, G. & Tóth, G. 2015. New generation of hydraulic pedotransfer functions for Europe. *European Journal of Soil Science*, **66**, 226–238.
- Tóth, G., Jones, A. & Montanarella, L. 2013. The LUCAS topsoil database and derived information on the regional variability of cropland topsoil properties in the European Union. *Environmental Monitoring & Assessment*, **185**, 7409–7425.
- Vandecasteele, B. & De Vos, B. 2001. *Relationship between Soil Textural Fractions Determined by the Sieve-Pipette Method and Laser Diffraction*. IBW Bb R 2001.003, Instituut voor Bosbouw & Wildbeheer, Ministerie van de Vlaamse Gemeenschap, Geraardsbergen.
- Yang, X., Zhang, Q., Li, X., Jia, X., Wei, X. & Shao, M. 2015. Determination of soil texture by laser diffraction method. *Soil Science Society of America Journal*, **79**, 1556–1566.